metals

MDPI

Article

Additive Manufacturing of Hot-Forming Dies Using Laser Powder Bed Fusion and Wire Arc Direct Energy Deposition Technologies

Artem Alimov *, Alexander Sviridov, Benjamin Sydow, Felix Jensch and Sebastian Härtel

Department of Hybrid Manufacturing, Brandenburg University of Technology Cottbus-Senftenberg, Konrad-Wachsmann-Allee 17, 03046 Cottbus, Germany; sviridov@b-tu.de (A.S.); sydow@b-tu.de (B.S.); jensch@b-tu.de (F.J.); haertel@b-tu.de (S.H.)

* Correspondence: alimov@b-tu.de

Abstract: Additive technologies are now widely used for the production of complex precise parts and have high potential for the production of forming dies. In this work, hot-forming dies optimized for additive manufacturing were developed and produced with wire arc direct energy deposition (WA-DED) and laser powder bed fusion (L-PBF) technologies. The concept of lightweight hot-forming dies with a 2D-lattice structure was developed, which reduced the weight of each die by 56%, from 14.2 kg to 6.1 kg, in production using L-PBF. Maraging/precipitation-hardened steel 17-4PH was used as an alternative to traditional hot-working steels with slightly lower mechanical properties and a much higher processability in the additive manufacturing process. The workability of the manufactured dies was confirmed by forging tests on an industrial screw press.

Keywords: additive manufacturing; hot-forming dies; L-PBF; WA-DED; WAAM

Citation: Alimov, A.; Sviridov, A.; Sydow, B.; Jensch, F.; Härtel, S. Additive Manufacturing of Hot-Forming Dies Using Laser Powder Bed Fusion and Wire Arc Direct Energy Deposition Technologies. *Metals* **2023**, *13*, 1842. https://doi.org/10.3390/met13111842

Academic Editor: Mohammad Jahazi

Received: 6 October 2023
Revised: 23 October 2023
Accepted: 25 October 2023
Published: 2 November 2023

1. Introduction

Additive manufacturing (AM) technologies [1] currently play an important role in the metal processing industry along with traditional formative and subtractive technologies [2]. They are widely used for rapid prototyping, manufacturing individual parts and small-scale production [3]. AM is considered to substantially increase material utilization and reduce total production time as well as energy consumption compared to metal forming or casting [4]. The main fields of AM applications are the aerospace [5], energy [6] and automotive industries [7] as well as biomedicine [8]. The materials processed include steels, aluminum, titanium, nickel, cobalt, magnesium and copper alloys.

Currently, powder bed fusion (PBF) and direct energy deposition (DED) [9] are the most widespread additive manufacturing methods. An electric arc, laser, plasma or electron beam may be used as an energy source.

Laser powder bed fusion (L-PBF) allows the production of complex spatial parts via layer-by-layer selective laser melting. It facilitates near-net-shape manufacturing with one of the highest accuracies among the AM technologies [10]. The main drawback is the limited dimensions of the workspace and relatively low productivity.

Direct energy deposition is an additive manufacturing process in which focused thermal energy is used to fuse materials via melting as they are being deposited. DED processes can be divided into powder-based and wire-based processes, depending on the form of the additive material used [11]. Wire-based DED that uses an electric arc (WA-DED, formerly WAAM) has the highest productivity among the AM methods. It is thought that because of the utilization of an electrical arc, WA-DED leads to a high thermal load during processing [12] and a large heat-affected zone [13] and can therefore only be used to a limited extent. The powder-based laser direct energy deposition (L-DEDp) process causes much lower thermal stresses, can be easily controlled and is characterized by a

low dilution ratio [14]. The main disadvantage of L-DEDp is its relatively low process productivity. Wire-based L-DED (L-DED-wire) offers a higher deposition rate with lower shape accuracy and resolution and a higher heat input and dilution ratio (28–42% according Caiazzo et al. [15]) compared to L-DEDp [16]. Using a novel hot-wire-based L-DED, it is possible to reduce the dilution ratio by up to 5% [17].

Typically, AM methods are used to produce parts; however, the production of casting molds [18] and metal forming dies [19] has tremendous potential. Additive manufacturing has found many applications in the manufacture of sheet metal forming dies. Stache's thesis [20] describes the production of an X38CrMoV5-3 (DIN 1.2367) die for sheet metal forming–press-hardening process using L-DEDp. The study of X55CrMoWV4-3-2-1 and X65MoCrWV3-2-1 steels revealed a tendency to crack during processing.

Nycz et al. used high-productivity WA-DED (5.5 kg/h) for the production of a large-scale (180 kg) stamping die from Lincoln L-59 mild steel coated with AISI 410 alloy. L-DEDp has been extensively used to produce sheet metal forming–press-hardening dies with cooling channels, for example, in the studies by Müller et al. [21], Gebauer et al. [22], Cortina et al. [23] and Pujante et al. [24].

The production of hot-bulk-forming dies via additive manufacturing technology is not covered as extensively in the literature. Huskic et al. [25] showed that die tools made of 1.2709 using L-DEDp are capable of undergoing 500 hot-bulk-forging cycles. Junker et al. [26] described the L-DEDp manufacturing process of an X37CrMoV5-1 (DIN 1.2343) hot-bulk-forging die. The hybrid manufactured tool with a machined base part and an active element added via additive manufacturing was integrated into the batch production process, and its workability was proven.

Thus, the potential of additive manufacturing technologies for the production of hot-bulk-forming dies has not been fully exploited. Traditional hot-working steels exhibit many problems during the AM process, such as crack formation due to complex thermal processing cycles [27]. Maraging/precipitation-hardened (PH) steels [28] may be a good alternative with slightly lower mechanical properties and a much higher processability in additive manufacturing. Moreover, the design of the dies could be improved to reduce the weight and to comply with the requirements for parts in additive manufacturing. Reducing the weight would also lead to a decrease in the forming die production time.

Thus, the aim of this work was to design hot-bulk-forming dies suitable for additive manufacturing and to develop AM technologies for their production. A technology for the hot-forging of a part from EN AW-6060 was chosen to be investigated, and a die geometry was developed based on the simulation of manufacturing from 17-4PH steel using L-PBF and WA-DED methods. Additive manufacturing of forming dies was proven to be effective through trial forgings with an SMS SPPE 6.3 screw press.

2. Materials and Methods

2.1. Materials

Each investigated process utilized material in the needed form, particularly powder for L-PBF and wire for WA-DED. The material used in the L-PBF process was a 17-4PH (FeCr17Ni4, AISI 630, DIN 1.4548) powder with a 20–45 µm particle size provided by m4p material solutions GmbH, Magdeburg, Germany. The wire used for WA-DED with a 1.2 mm diameter made of17-4PH (FeCr17Ni4, AISI 630, DIN 1.4548) was provided by Metal Technology Canterbo GmbH, Meerbusch, Germany. The chemical composition is presented in Table 1.

Table 1. Chemical composition of the 17-4PH powder.

Element	Cr	Ni	Cu	Nb	C	Si	Mn	Fe
Nom.	15.0–17.0	3.0–5.0	3.0–5.0	0.15–0.45	<0.07	<1.00	<0.70	Bal.
L-PBF	16.0	4.0	4.0	0.29	0.03	0.60	0.70	
WA-DED	16.37	4.78	3.63	0.23	0.019	0.46	0.64	

Workpieces were made from AlMgSi (EN-AW 6060, DIN 3.3206) D80x6000 mm bars provided by Gemmel Metalle GmbH, Berlin, Germany. The chemical composition is presented in Table 2.

Table 2. The chemical composition of the AlMgSi bars.

Element	Mg	Si	Fe	Cu	Mn	Ti	Zn	Al
Nom.	0.35–0.60	0.30–0.60	0.10–0.30	<0.10	<0.10	<0.10	<0.15	Bal.
Fact.	0.436	0.596	0.186	0.004	0.012	0.015	0.003	

2.2. Forging

Forging was performed on an SMS SPPE 6.3 screw press (SMS group GmbH, Düsseldorf, Germany) with a nominal force of 6.3 MN. The maximum speed of the ram was 700 mm/s. The nominal impact energy was 14 kJ. The actual impact energy was controlled by adjusting the ram speed accordingly. The upper and lower dies were installed in the press with a die holder using an adapter and aligned to ensure the absence of offset or twist. The die holder was equipped with prism slides.

The workpieces were manufactured on a CNC turning lathe according to the drawing. Before forging, the workpieces were sprayed with a water-based hexagonal boron nitride lubricant, air-dried, placed in a chamber furnace at 480 °C and heated for 1.5 h. The workpieces were then transferred manually from the furnace to the dies using forging tongs. Forging was performed in semiautomatic mode with 3 blows with a pause of 2 s between blows. The forgings were also extracted manually using forging tongs.

2.3. WA-DED

The WA-DED process was realized on a GEFERTEC arc605 machine (Gefertec GmbH, Berlin, Germany) with a Fronius TPS400i (Fronius Deutschland GmbH, Berlin, Germany) welding power source (Figure 1a). The WA-DED parameters were determined with preliminary trials. Parameters were chosen based on good bonding of adjacent beads and a stable process. ArC2 (argon + 2% carbon dioxide with a flow rate of 15 L/min) was used as the shielding gas. The stickout (contact nozzle-to-workpiece distance) was 15 mm. The substrate was a C45 W round disc (Figure 1b) with dimensions of Ø238 mm × 60 mm, which was not preheated. Both die halves were produced parallel to the process acceleration. During the entire WA-DED process runtime, local compressed-air cooling of the surface took place after each welding layer at the next point to be welded until the temperature at this position fell below 150 °C. The temperature was measured during the process using a pyrometer with an emission coefficient set to 1.

(**a**) (**b**)

Figure 1. WA-DED machine GEFERTEC arc605 (**a**) and a photo taken during the manufacturing process (**b**).

2.4. L-PBF

An EOS M290 (EOS GmbH, Krailling, Germany) was used to produce the forging dies via L-PBF technology (Figure 2a). This machine uses a 400 W laser, which is focused to a diameter of 80 µm in the printing area. The L-PBF parameters were provided by the machine manufacturer. Production was carried out at a laser power of approx. 220 W, an exposure speed of approx. 750 mm/s, a hatching distance of 0.11 mm, a substrate plate temperature of 80 °C and a layer thickness of 40 µm (Figure 2b). The part was fabricated directly on the build plate without any support structures to avoid warpage. The part was subsequently separated from the substrate plate via wire-cut EDM. To obtain a surface suitable for forging, the rough surface was processed from the as-printed state via milling.

(**a**) (**b**)

Figure 2. LPB-F machine EOS M290 (**a**) and a photo taken during the manufacturing process (**b**).

2.5. Forging Simulation

Simulations were performed with the commercial FEM software QForm UK 10.2.4 (QForm Group FZ LLC, Fujairah, United Arab Emirates) in a general forming module. The workpiece was set as an elastic–plastic body, and the tools were set as rigid bodies. The die mesh consisted of approximately 170,000 volumetric finite elements, while the workpiece mesh at the end of the forging consisted of approximately 300,000 volumetric finite elements. Remeshing of the workpiece was performed automatically. The maximum strain increment on a step was 0.1. The equipment used in the simulation was a screw press with a nominal impact energy of 14 kJ and a nominal force of 6.3 MN. Stamping was simulated in 3 blows with full energy. The maximum speed of the ram was 700 mm/s. Thermal processes were also considered. The initial temperature of the workpiece was set as 480 °C with subsequent air cooling for 2 s and cooling in dies for 1 s. The initial temperature of the dies was set as 20 °C. Friction was set by a shear law with m = 0.4. Heat transfer coefficient was set as 40,000 W/(m^2·K) with a pause coefficient of 0.05. The flow curves and thermophysical parameters of the workpiece and the dies were set according to the EN AW-6060 and H11 (EN 1.2343) steels from the QForm standard database, respectively. The environment was set as "Air" from the QForm standard database.

The geometry models used in the simulation are shown in Figure 3.

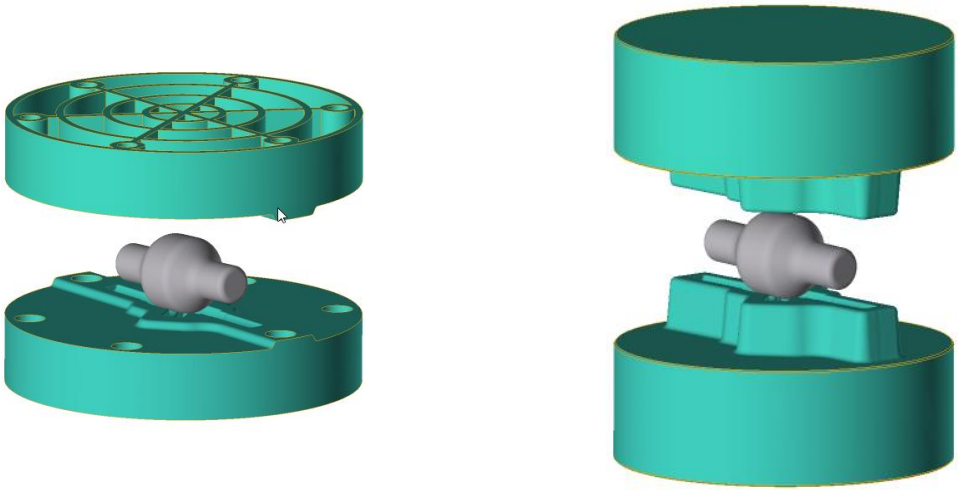

(**a**) (**b**)

Figure 3. The geometry models used in the forging simulation with L-PBF (**a**) and WA-DED (**b**) dies.

3. Results

3.1. Simulation of the Forging Process and Die Analysis

To develop a defect-free forging technology, an iterative simulation procedure with QFORM was performed, and the geometry of the forged part and the workpiece was designed (Figure 4). Elements of the finished part (Figure 4a) that could not be obtained with stamping, such as small holes and grooves, were filled with material to obtain the forged part (Figure 4b) geometry. The use of a twin forged part (Figure 4c) made it possible to significantly increase the metal consumption and forgeability of the part by increasing the thickness of the flange.

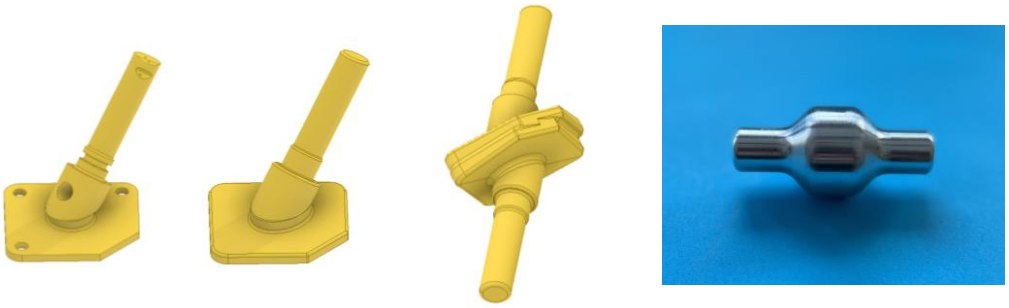

(**a**) (**b**) (**c**) (**d**)

Figure 4. The geometry of the finished (**a**), forged (**b**), twin forged (**c**) parts and the workpiece (**d**).

An analysis of the metal flow during the forging process was performed using WA-DED forging dies (Figure 5). Since the forging dies made using L-PBF had the same impression geometry, the metal flow was similar. The first step of forging is upsetting the workpiece with a predominantly lateral material flow. As the distance between the dies decreases and the flash surface increases, the resistance to lateral material flow increases, and the rising phase begins, followed by the filling of deep die cavities. As seen in the figure, in the final stage of forging, the entire surface of the workpiece came into contact with the tool, indicating that there was no underfilling. The simulation also showed that there were no defects, such as folds.

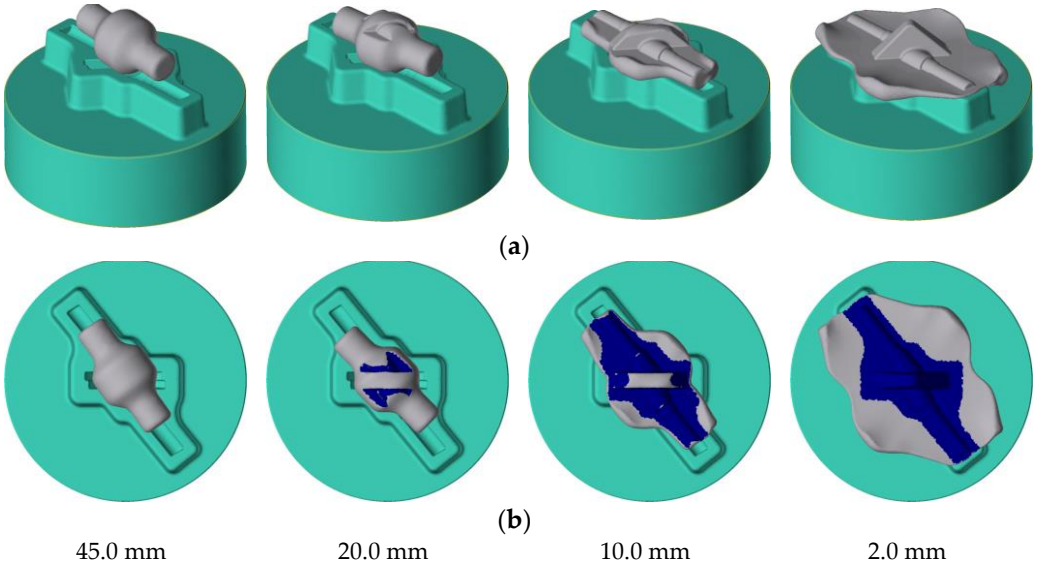

Figure 5. Metal flow during forging (**a**), contact zones between the workpiece and the dies (**b**) and the distance between the dies.

Analysis of the simulation results showed that the temperature in the workpiece (Figure 6) did not exceed 500 °C, which ensured the absence of metallurgical defects and a high level of mechanical properties. There was a small area in the flash with temperatures above 500 °C, but this was to be removed and had no effect on the forging.

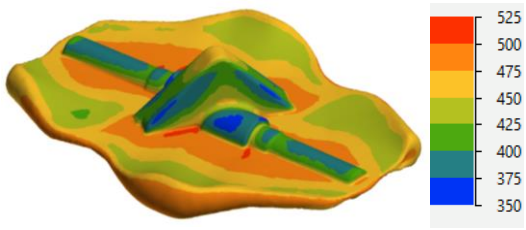

Figure 6. Temperature distribution in the workpiece after hot forging.

The temperature distribution in the dies was also analyzed using the QForm cyclic tool heating module. A simulation of the forging process was carried out with a pause of 10 s between forgings before stabilizing the die temperature after forging. This simulation allowed us to analyze the actual die temperature during continuous forging of several parts. As shown in Figure 7, the surface temperature of the WA-DED-manufactured die was approximately 160 °C in the cavity and 255 °C at the radius of the shaft, while that of the L-PBF-manufactured die was approximately 200 °C in the cavity and 280 °C at the radius of the shaft. The higher die temperature of the L-PBF-produced die was caused by the reduced heat transfer from the die impression due to the hollow die geometry.

Analysis of the effective stresses shown in Figure 8 revealed that the L-PBF-produced die also had higher stresses up to 1000–1200 MPa in contrast to the WA-DED-produced die, which had stresses up to 900–1050 MPa. The maximum stresses in both cases occurred at the corner of the cavities forming the flange of the twin forgings. It should also be mentioned that these stresses were mostly tensile and may have led to cracking in these areas.

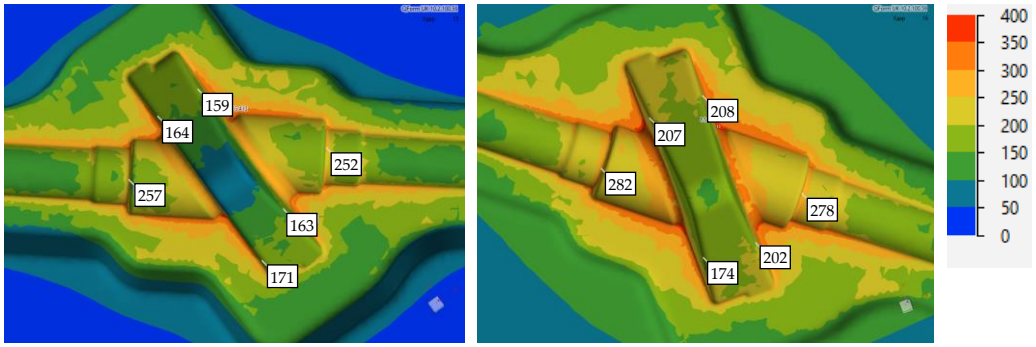

(**a**) (**b**)

Figure 7. Temperature distribution on the die surface during the forging with WA-DED (**a**) and L-PBF (**b**) made dies after cyclic tool heating.

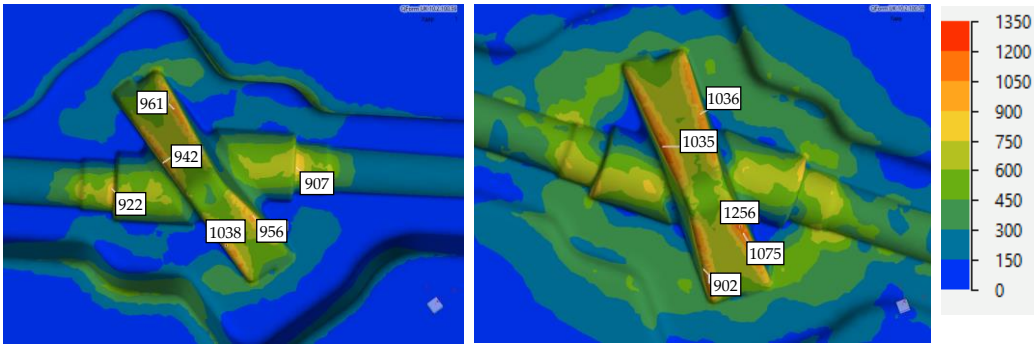

(**a**) (**b**)

Figure 8. Effective stress distribution on the die surface during the forging with WA-DED (**a**) and L-PBF (**b**) made dies.

3.2. Design of Hot-Forming Dies for Additive and Hybrid Manufacturing

The forming dies were designed in such a way that the advantages of the selected manufacturing processes were used in the best possible way. A substrate plate of C45 steel (EN 1.0503) was used to manufacture the tools using WA-DED (Figure 9a), onto which 17-4PH steel (EN 1.4542) was applied with a stock allowance and without die impression. Further heat treatment and machining were carried out to achieve the desired die impression geometry and the necessary mechanical properties.

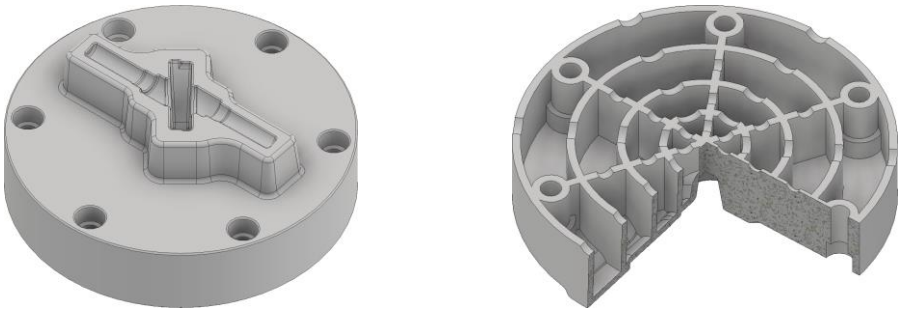

(**a**) (**b**)

Figure 9. Design of the forming dies for the production with WA-DED (**a**) and L-PBF (**b**) technologies.

As the production of solid components using the L-PBF process is challenging, the dies were designed as a 2D-lattice structure (Figure 9b). In addition to the reduced manufacturing time and the reduced distortion, the weight of each tool was reduced by 56%,

from 14.2 kg to 6.1 kg. After manufacturing with the L-PBF process with the die impression including a 0.5 mm stock allowance, the working surface of the tools was milled. The approach used significantly shortened the machining time and simplified the milling work considerably. Since the bearing surface area due to the 2D-lattice structure was significantly smaller than that of WA-DED-produced dies, it was necessary to use hardened underlayers to prevent plastic deformation of the die holder and subsequent deformation of the die inserts.

3.3. Manufacturing Process

For the production of the forging dies with the WA-DED process, path planning was realized in such a way that both die halves were produced in parallel to utilize the natural cooling of the tool half that was not being welded and thus minimize the process time. The meander geometry with a transverse alignment was used as a deposition strategy to enable a mostly continuous WA-DED process (Figure 10), which means that only one start and end point was needed for each welding layer. The wire feed speed was v_f = 7.0 m/min, and the welding speed was v_w = 400 mm/min. The seam width was 7.5 mm, and the bead-to-bead distance was 4.2 mm (corresponding to a bead overlap of approx. 0.44). Ten layers were applied with a Z offset of 3.5 mm/layer.

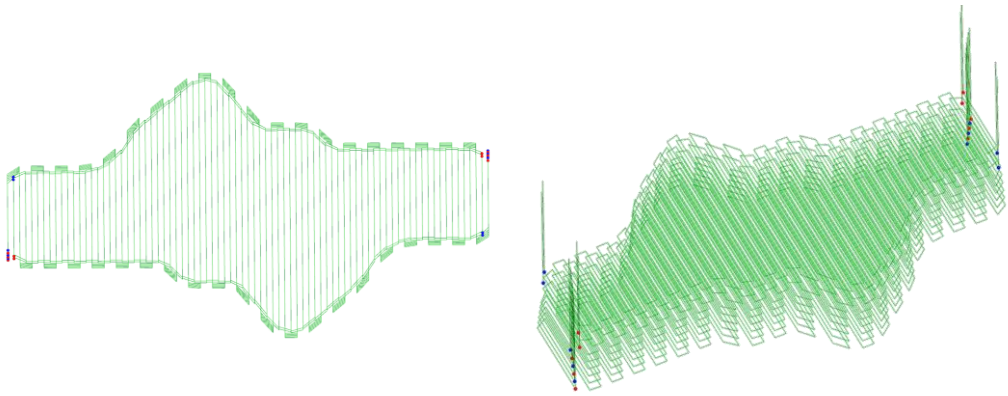

(**a**) (**b**)

Figure 10. Top (**a**) and isometric (**b**) views of WA-DED weld path planning.

The WA-DED process was stable during the whole process. From the third layer onwards, it became apparent that the end areas tended to overheat, which led to melt running. This leads to the formation of slopes, which are unfavorable for the further welding process (Figure 11—the eighth layer is shown as an example). These slopes were compensated for by depositing an additional local welding layer on the incompletely filled areas to create a flat surface at the end areas. No other welding defects occurred during the WA-DED process.

The raw parts of both forming die halves were successfully produced using WA-DED with compensation for the defect areas (Figure 12a). The total WA-DED process time, including cooling times, was approx. 3 h for the production of both forming die halves simultaneously. The wire consumption was approximately 4 kg. Machining took place without cracking. A machined die half (without mounting elements) is shown in Figure 12b. The obtained machined die surface was technically smooth and free of defects (binding defects, pores).

The deposition strategy used in L-PBF manufacturing was meander-shaped exposure in 12 mm wide strips with a 47° strip rotation from layer to layer (Figure 13). Complete exposure of one strip was performed before the transition to the next strip. This deposition strategy ensures a low probability of joint defects as well as high mechanical properties and minimization of anisotropy.

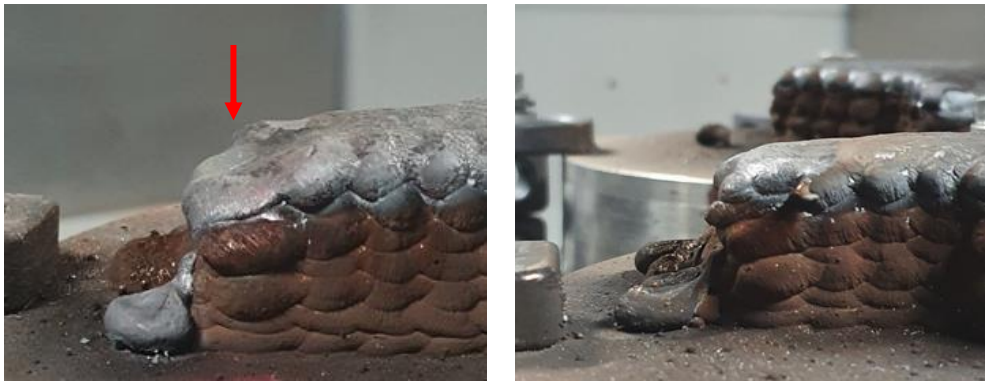

(**a**) (**b**)

Figure 11. The welding defect (**a**, red arrow) and its compensation using an additional local welding layer (**b**).

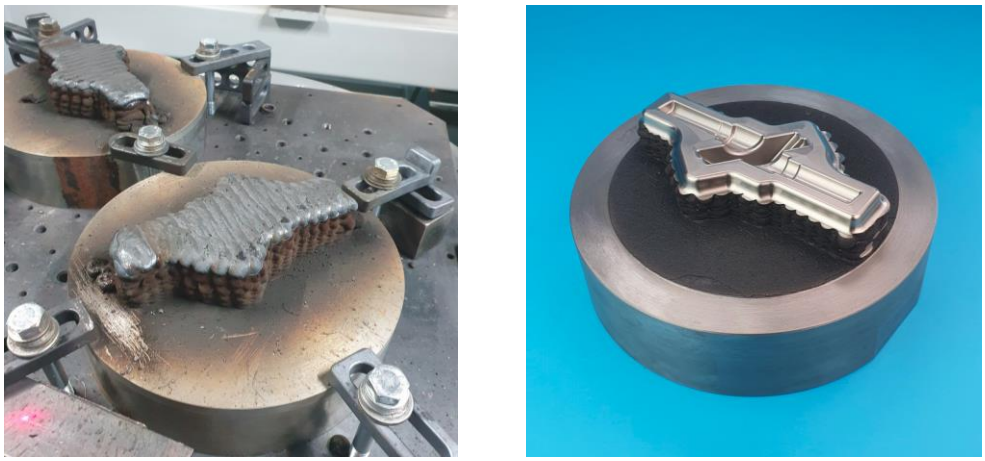

(**a**) (**b**)

Figure 12. Finished WA-DED parts (**a**) and the forming die after machining (**b**).

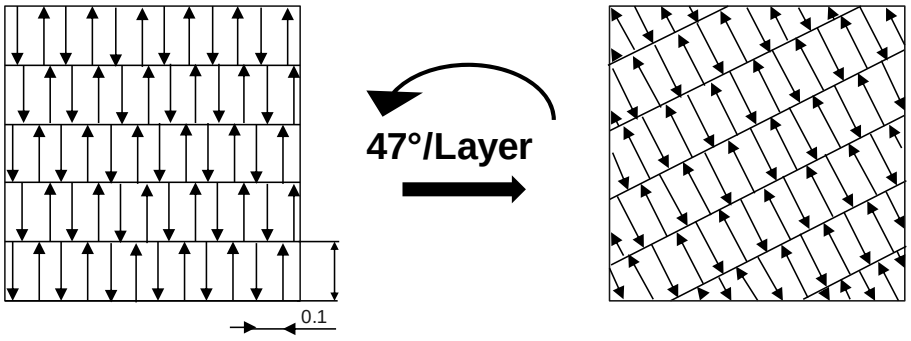

Figure 13. Deposition strategy used in L-PBF manufacturing.

The production time of each forming die half was 76 h, and the process was completed without incident (Figure 14).

The actual impression geometries of the L-PBF-produced dies were compared with target CAD geometries. For this purpose, they were scanned using the industrial 3D optical measurement system GOM Atos 5 (Carl Zeiss GOM Metrology GmbH, Braunschweig, Germany). The scans were further analyzed using GOM ATOS 2020 software (Carl Zeiss GOM Metrology GmbH, Braunschweig, Germany) Deviation maps are presented in Figure 15. The deviation analysis showed that the maximum deviation reached −0.34 mm in the rod

length. The standard deviation was 0.09 mm for both die parts. Thus, machining with a 0.5 mm stock removal will produce the target die impression geometry.

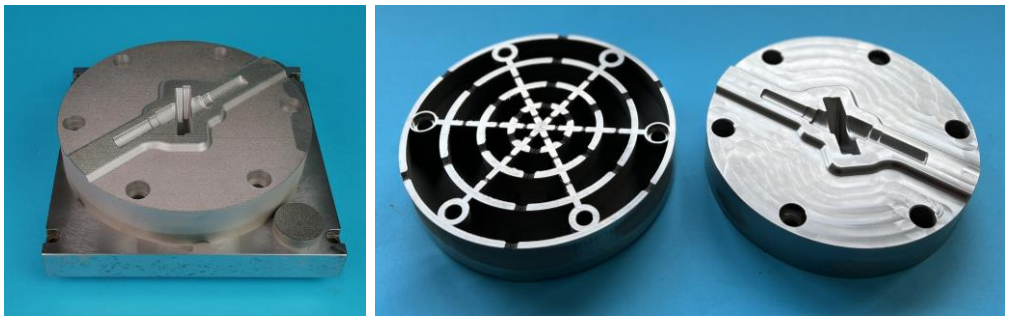

(**a**) (**b**)

Figure 14. Finished L-PBF part (**a**) and the forming dies after machining (**b**).

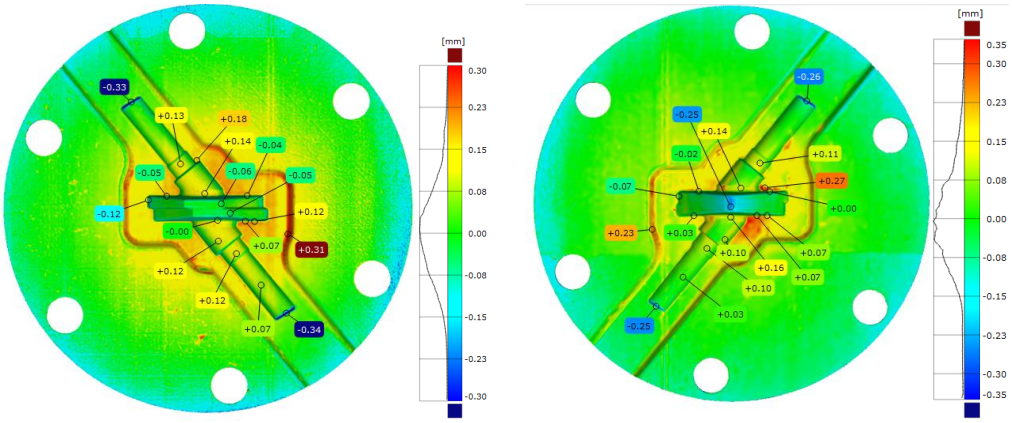

(**a**) (**b**)

Figure 15. Deviation maps of the L-PBF-produced top (**a**) and bottom (**b**) dies.

Since the L-PBF-produced forging dies were provided with finished impressions with a stock to be machined to only 0.5 mm, the milling time was reduced from 80 h for both WA-DED-produced dies to 30 h for both L-PBF-produced dies.

3.4. Forging Trials

The hot-forming dies were mounted on the SMS SPPE 6.3 screw press. The assembly of WA-DED-manufactured tools in the press is shown in Figure 16. The WA-DED-manufactured forging die inserts were fastened with bolts in the adapter, which was fixed with clamps to the die holder.

The effect of the blow energy and number of blows on the forging process was investigated. The fraction of full-impact energy was varied during the hot-forming process as follows: 50%, 70% and 100%, two blows with 100% and three blows with 100%. In Figure 17, the effect of the fraction of full-impact energy and the number of blows on the workpiece's plastic deformation is shown. The forming stages and final shape of the forging correspond very well with those predicted in the simulation.

The assembly of the L-PBF-manufactured forming dies in the press and the manufactured forged part are shown in Figure 18. The L-PBF-manufactured forging die inserts were fastened in the same way as the WA-DED-produced dies.

As shown in Figure 18, complete filling of the die cavity with flash formation along the entire contour of the workpiece occurred during forging. Defects such as folds were not present. With each set of dies, ten forgings were made, and no signs of wear, damage or warping of the dies were detected.

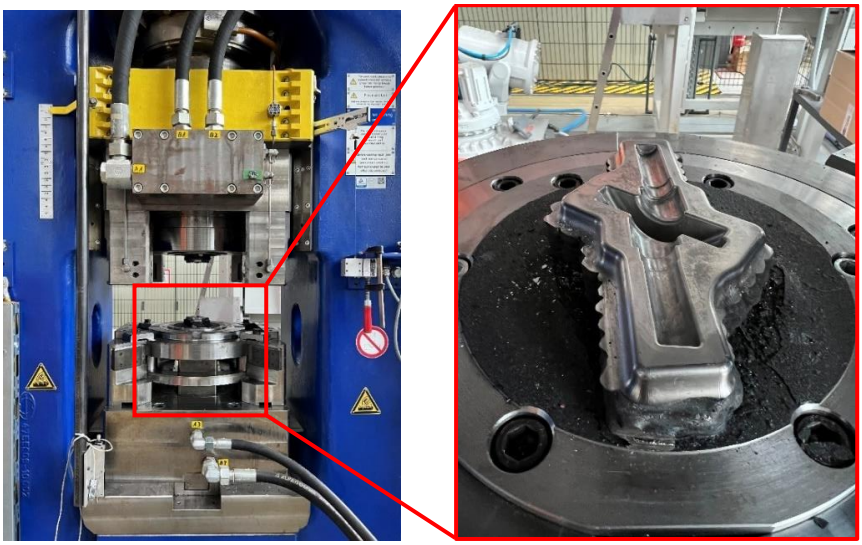

Figure 16. Assembly of WA-DED-manufactured tools in the press.

Blow energy	50%	70%	100%	100%	100%
Blows	1	1	1	2	3
Flash thickness	7.9	7.2	7.1	3.9	2.1

Figure 17. Experimental investigation of the forging process.

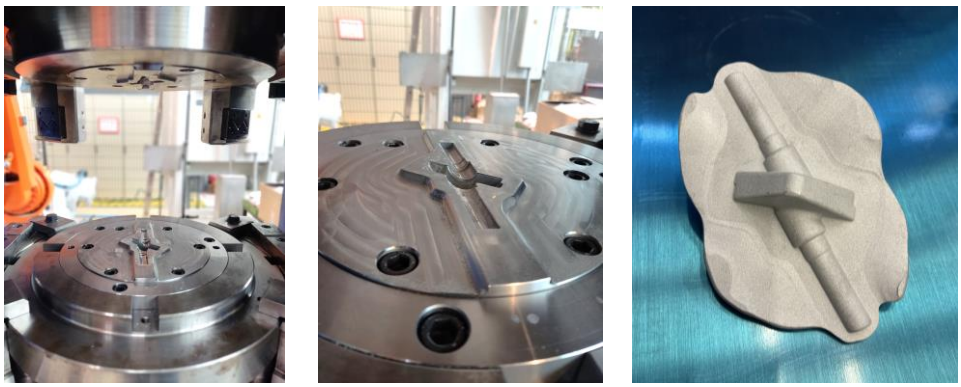

(**a**) (**b**) (**c**)

Figure 18. Assembly of the L-PBF manufactured dies mounted in the press (**a**) with a die holder (**b**) and the forged part (**c**).

4. Discussion

At present, the interest of the scientific and industrial community in the use of additive technologies for die manufacturing [19] and repair [29] is quite high. Making dies contributes significantly to the cost of forged parts. In addition, the die-making process is time-consuming and requires considerable equipment for machining and heat treatment. Additive technologies have significant potential to accelerate and reduce the cost of die production, especially for individual and small batch forging, where metal forming may

not be cost-effective at all compared to other manufacturing methods such as casting and machining. There are a considerable number of works devoted to the additive manufacturing of forming dies, especially for die stamping [21,23], as covered in the Introduction. However, the direct use of die steels for additive manufacturing has significant constraints. Due to complex thermal loading, die steels exhibit poor processability in additive manufacturing, and no ready-to-use solutions have been presented in the literature thus far. Most researchers are trying to utilize traditional die steels for additive die manufacturing [20,25,26], using various technical solutions such as the use of preheated substrate to prevent defects like hot cracks. A method for the hybrid production of dies has also been proposed wherein only individual elements of the die working surfaces are produced using additive manufacturing [30,31]. In this case, by reducing the volume of deposited metal, residual stresses and, consequently, the risk of defects, are reduced. In this paper, we propose another approach, namely, using steel suitable for additive manufacturing, particularly 17-4PH for die production. Using this steel allows hot-forging dies to be produced without defects. Additive manufacturing material suppliers also offer other tool steels that are of great interest for die manufacturing, such as MS1 (1.2709), CX and CM55. These steels have some lower mechanical properties compared to die steels, as well as lower operating temperatures. However, the question of their use for the production of forging dies for prototyping, individual and small batch forging remains open.

In most of the work described above, the laser direct energy deposition method (L-DED) was used to fabricate hot-stamping dies. In this paper, two other additive manufacturing processes, WA-DED and L-PBF, were investigated. WA-DED is characterized by a higher production rate, but the near-net-shape manufacturing capabilities of this method are limited, and a complex deep die cavity cannot be produced. Additionally, due to higher thermal loads, crack formation and warping of the manufactured parts are more likely to occur [32]. The L-PBF method is characterized by significantly lower heat input and high accuracy, which makes it possible to produce dies with impressions with a stack to be machined to only 0.3–0.5 mm. In addition, through the use of a 2D-lattice structure design, the weight of each tool was reduced by 56%, from 14.2 kg to 6.1 kg, in production via L-PBF. Compared to the conventional solid die manufacturing approach [26], this will reduce internal stresses and the probability of cracking.

Since dies are subjected to high thermomechanical loads during the forging process. Further research is essential to investigate the potential of additively manufactured dies for use in industrial applications. There is quite extensive research available on conventionally produced 17-4PH steel [33]. However, the mechanical properties of additively manufactured 17-4PH steel have not been widely investigated. The fatigue performance of 17-4PH was investigated primarily in high-cycle (HCF) and in low-cycle fatigue (LCF) modes without heat treatment [34] as well as with an H1100 heat treatment [35]. LCF with the heat treatment designation H900, which is most appropriate for die production, has not been investigated. The fracture toughness of additively manufactured dies should also be investigated. It is also necessary to investigate the creep resistance of these steels, as the maximal operating temperature is much lower than that of die steels.

5. Conclusions

In this work, weight-optimized hot-bulk-forming dies suitable for additive manufacturing were designed, and AM technologies for their production were developed. Two processes were investigated: L-PBF and WA-DED. Summarizing the following findings, we can conclude:

1. WA-DED is characterized by a higher production rate, but the near-net-shape manufacturing capabilities of this method are limited, and a complex deep die cavity cannot be produced.
2. The L-PBF method makes it possible to produce dies with impressions with a stock to be machined to only 0.3–0.5 mm.

3. Through the use of a 2D-lattice structure, the weight of each tool was reduced by 56%, from 14.2 kg to 6.1 kg, in production via L-PBF.
4. The forging process was simulated, and the die temperature and stresses were analyzed.
5. Additive manufacturing of the forming dies was proven through trial forgings to be effective.
6. The fatigue life, fracture toughness, creep resistance and wear behavior of the additive-manufactured forming dies as well as the possibility of their use in industrial applications should be further investigated.

Author Contributions: A.A.: Conceptualization, Methodology, Investigation, Visualization, Writing—Original Draft, Writing—Review and Editing. A.S.: Conceptualization, Resources, Supervision, Project Administration, Funding Acquisition, Writing—Review and Editing. B.S.: Investigation, Visualization, Writing—Original Draft. F.J.: Investigation, Visualization, Writing—Original Draft. S.H.: Resources, Supervision, Project Administration, Writing—Review and Editing. All authors have read and agreed to the published version of the manuscript.

Funding: This work was supported by the European Union and the European Regional Development Fund and was carried out in the framework of the project GABRIEL—Erforschung GAnzheitlicher, HyBrid-ElektRIscher AntriebskomponEnten für die Luftfahrt (ProFIT Brandenburg, Application number: 80257607).

Data Availability Statement: The data presented in this study are available on request from the corresponding author.

Acknowledgments: We acknowledge the support by the German Research Foundation and the BTU Cottbus-Senftenberg.

Conflicts of Interest: The authors declare no conflict of interest.

References

1. Redwood, B.; Schöffer, F.; Garret, B. *The 3D Printing Handbook: Technologies, Design and Applications*; 3D Hubs: Amsterdam, The Netherlands, 2017.
2. Popov, V.V.; Fleisher, A. Hybrid Additive Manufacturing of Steels and Alloys. *Manuf. Rev.* **2020**, *7*, 6. [CrossRef]
3. Liu, G.; Zhang, X.; Chen, X.; He, Y.; Cheng, L.; Huo, M.; Yin, J.; Hao, F.; Chen, S.; Wang, P.; et al. Additive Manufacturing of Structural Materials. *Mater. Sci. Eng. R Rep.* **2021**, *145*, 100596. [CrossRef]
4. Rasiya, G.; Shukla, A.; Saran, K. Additive Manufacturing—A Review. *Mater. Today Proc.* **2021**, *47*, 6896–6901. [CrossRef]
5. Gisario, A.; Kazarian, M.; Martina, F.; Mehrpouya, M. Metal Additive Manufacturing in the Commercial Aviation Industry: A Review. *J. Manuf. Syst.* **2019**, *53*, 124–149. [CrossRef]
6. Sun, C.; Wang, Y.; McMurtrey, M.D.; Jerred, N.D.; Liou, F.; Li, J. Additive Manufacturing for Energy: A Review. *Appl. Energy* **2021**, *282*, 116041. [CrossRef]
7. Scholz, S.G.; Howlett, R.J.; Setchi, R. (Eds.) *Sustainable Design and Manufacturing: Proceedings of the 8th International Conference on Sustainable Design and Manufacturing (KES-SDM 2021)*; Smart Innovation, Systems and Technologies; Springer: Singapore, 2022; Volume 262, ISBN 9789811661273.
8. Sheoran, A.J.; Kumar, H.; Arora, P.K.; Moona, G. Bio-Medical Applications of Additive Manufacturing: A Review. *Procedia Manuf.* **2020**, *51*, 663–670. [CrossRef]
9. *DIN EN ISO/ASTM 52900:2022-03*; Additive Fertigung—Grundlagen—Terminologie; Deutsche Fassung EN ISO/ASTM 52900:2021. Beuth Verlag GmbH: Berlin, Germany, 2022.
10. Sing, S.L.; Yeong, W.Y. Laser Powder Bed Fusion for Metal Additive Manufacturing: Perspectives on Recent Developments. *Virtual Phys. Prototyp.* **2020**, *15*, 359–370. [CrossRef]
11. Kisielewicz, A.; Thalavai Pandian, K.; Sthen, D.; Hagqvist, P.; Valiente Bermejo, M.A.; Sikström, F.; Ancona, A. Hot-Wire Laser-Directed Energy Deposition: Process Characteristics and Benefits of Resistive Pre-Heating of the Feedstock Wire. *Metals* **2021**, *11*, 634. [CrossRef]
12. Ayed, A.; Valencia, A.; Bras, G.; Bernard, H.; Michaud, P.; Balcaen, Y.; Alexis, J. Effects of WAAM Process Parameters on Metallurgical and Mechanical Properties of Ti-6Al-4V Deposits. In *Advances in Materials, Mechanics and Manufacturing*; Chaari, F., Barkallah, M., Bouguecha, A., Zouari, B., Khabou, M.T., Kchaou, M., Haddar, M., Eds.; Lecture Notes in Mechanical Engineering; Springer International Publishing: Cham, Switzerland, 2020; pp. 26–35, ISBN 978-3-030-24246-6.
13. Benakis, M.; Costanzo, D.; Patran, A. Current Mode Effects on Weld Bead Geometry and Heat Affected Zone in Pulsed Wire Arc Additive Manufacturing of Ti-6-4 and Inconel 718. *J. Manuf. Process.* **2020**, *60*, 61–74. [CrossRef]
14. Güpner, M.; Rochholz, C.; Bliedtner, J.; Zeidler, H. Process Characterization in Laser Metal Deposition of Hot Work Tool Steel. In Proceedings of the 11th CIRP Conference on Photonic Technologies [LANE 2020], Fürth, Germany, 7–10 September 2020.

15. Caiazzo, F.; Alfieri, V. Directed Energy Deposition of Stainless Steel Wire with Laser Beam: Evaluation of Geometry and Affection Depth. *Procedia CIRP* **2021**, *99*, 348–351. [CrossRef]
16. Ding, D.; Pan, Z.; Cuiuri, D.; Li, H. Wire-Feed Additive Manufacturing of Metal Components: Technologies, Developments and Future Interests. *Int. J. Adv. Manuf. Technol.* **2015**, *81*, 465–481. [CrossRef]
17. Tyralla, D.; Freiße, H.; Seefeld, T.; Thomy, C.; Dreher, M.; Schnick, M.; Narita, R. Laser Hot Wire Cladding (LHWC) with Single and Multiple Wires for High Deposition Rates and Low Dilution. *Weld. Cut.* **2020**, *19*, 220–226.
18. Gao, M.; Li, L.; Wang, Q.; Ma, Z.; Li, X.; Liu, Z. Integration of Additive Manufacturing in Casting: Advances, Challenges, and Prospects. *Int. J. Precis. Eng. Manuf.-Green Tech.* **2022**, *9*, 305–322. [CrossRef]
19. Chantzis, D.; Liu, X.; Politis, D.J.; El Fakir, O.; Chua, T.Y.; Shi, Z.; Wang, L. Review on Additive Manufacturing of Tooling for Hot Stamping. *Int. J. Adv. Manuf. Technol.* **2020**, *109*, 87–107. [CrossRef]
20. Stache, R. Untersuchungen Zur Herstellung von Werkzeugelementen Für Das Presshärten Mittels Laser Beam Melting. Ph.D. Thesis, Technische Universität Chemnitz, Chemnitz, Germany, 2020.
21. Müller, B.; Gebauer, M.; Malek, R.; Gerth, N. Metal Additive Manufacturing for tooling applications-Laser Beam Melting technology increases efficiency of dies and molds. In Proceedings of the Metal Additive Manufacturing Conference MAMC, Vienna, Austria, 20–21 November 2014.
22. Gebauer, M.; Stoll, P.; Müller, B.; Spierings, A.; Polster, S.; Feld, T.; Klinger, M.; Zurbrügg, A. High Performance Sheet Metal Forming Tooling by Additive Manufacturing. In *iCAT 2016, Proceedings of the 6th International Conference on Additive Technologies, Nürnberg, Germany, 29–30 November 2016*; Interesana-zavod: Ljubljana, Slovenia, 2016. [CrossRef]
23. Cortina, M.; Arrizubieta, J.; Calleja, A.; Ukar, E.; Alberdi, A. Case Study to Illustrate the Potential of Conformal Cooling Channels for Hot Stamping Dies Manufactured Using Hybrid Process of Laser Metal Deposition (LMD) and Milling. *Metals* **2018**, *8*, 102. [CrossRef]
24. Pujante, J.; González, B.; Garcia-Llamas, E. Pilot Demonstration of Hot Sheet Metal Forming Using 3D Printed Dies. *Materials* **2021**, *14*, 5695. [CrossRef]
25. Huskic, A.; Behrens, B.; Giedenbacher, J.; Huskic, A. Standzeituntersuchungen Generativ Hergestellter Schmiedewerkzeuge. *Schmiede J.* **2013**, *92013*, 66–70.
26. Junker, D.; Hentschel, O.; Schramme, R.; Schmidt, M.; Merklein, M. Performance of Hot Forging Tools Built by Laser Metal Deposition of Hot Work Tool Steel X37CrMoV5-1. In Proceedings of the Laser in Manufacturing Conference, Munich, Germany, 26–29 June 2017.
27. Frazier, W.E. Metal Additive Manufacturing: A Review. *J. Mater. Eng Perform* **2014**, *23*, 1917–1928. [CrossRef]
28. Haghdadi, N.; Laleh, M.; Moyle, M.; Primig, S. Additive Manufacturing of Steels: A Review of Achievements and Challenges. *J. Mater. Sci.* **2021**, *56*, 64–107. [CrossRef]
29. Foster, J.; Cullen, C.; Fitzpatrick, S.; Payne, G.; Hall, L.; Marashi, J. Remanufacture of Hot Forging Tools and Dies Using Laser Metal Deposition with Powder and a Hard-Facing Alloy Stellite 21®. *J. Remanuf.* **2019**, *9*, 189–203. [CrossRef]
30. Meiners, F.; Ihne, J.; Jürgens, P.; Hemes, S.; Mathes, M.; Sizova, I.; Bambach, M.; Hama-Saleh, R.; Weisheit, A. New Hybrid Manufacturing Routes Combining Forging and Additive Manufacturing to Efficiently Produce High Performance Components from Ti-6Al-4V. *Procedia Manuf.* **2020**, *47*, 261–267. [CrossRef]
31. Bambach, M.; Sizova, I.; Sviridov, A.; Stendal, J.; Günther, M. Batch Processing in Preassembled Die Sets—A New Process Design for Isothermal Forging of Titanium Aluminides. *JMMP* **2018**, *2*, 1. [CrossRef]
32. Kempen, K.; Vrancken, B.; Buls, S.; Thijs, L.; Van Humbeeck, J.; Kruth, J.-P. Selective Laser Melting of Crack-Free High Density M2 High Speed Steel Parts by Baseplate Preheating. *J. Manuf. Sci. Eng.* **2014**, *136*, 061026. [CrossRef]
33. Rack, H.J.; Kalish, D. The Strength, Fracture Toughness, and Low Cycle Fatigue Behavior of 17-4 PH Stainless Steel. *Met. Trans.* **1974**, *5*, 1595–1605. [CrossRef]
34. Concli, F.; Fraccaroli, L.; Nalli, F.; Cortese, L. High and Low-Cycle-Fatigue Properties of 17–4 PH Manufactured via Selective Laser Melting in as-Built, Machined and Hipped Conditions. *Prog. Addit. Manuf.* **2022**, *7*, 99–109. [CrossRef]
35. Carneiro, L.; Jalalahmadi, B.; Ashtekar, A.; Jiang, Y. Cyclic Deformation and Fatigue Behavior of Additively Manufactured 17–4 PH Stainless Steel. *Int. J. Fatigue* **2019**, *123*, 22–30. [CrossRef]